

Creep deformation behaviour of Rhenium free Ni-based single crystal superalloys LSC-15

Nobuyasu Tsuno^a and Satoshi Takahashi

IHI Corporation, Research Laboratory, 1 Shin-nakahara-cho, Isogo-ku, Yokohama, Japan

Abstract. In this paper, creep deformation behavior of Ni-based single crystal superalloys LSC-15 were studied. LSC-15 does not include Rhenium and has been developed by IHI Corporation Japan. Creep tests were performed at 1000 and 1050 °C under several stress levels. The creep deformation behaviour was different between test temperatures at 1000 °C and 1050 °C. Moreover, the relationship between the minimum creep rate and stress was different at the various temperatures. The stress exponent values at 1000 °C and 1050 °C, were $n = 6$ and 12 respectively. This difference was due to differences in the formation of dislocation network. At 1000 °C, when the minimum creep rate, the dislocation network formed completely independent of stress level. On the other hand, at 1050 °C, the dislocation network had not developed fully at the minimum creep rate and the formation of dislocation network depended on the stress level. Therefore, stress dependency at 1050 °C is higher than that at 1000 °C.

1. Introduction

Gas turbine components require thermal fatigue and creep resistance at high temperature. In general, more refractory elements such as rhenium improve the creep resistance of the materials for advanced turbine blade [1–4]. It has also been reported that the γ/γ' rafting behaviour is effective for creep resistance in case of the single crystal (SX) superalloys [5,6]. However, the price of rhenium, which is primarily consumed for the production of nickel base superalloys, has been substantially increasing for several years. To overcome these situations, several researchers have attempted to develop SX superalloys with the lower rhenium content which has the same level of creep resistance as the second generation superalloys with rhenium [7,8]. In Japan, IHI Corporation developed the Re-free SX superalloy. The high γ/γ' lattice misfit of this alloy improves the high temperature creep strength even though the alloy does not include rhenium. Therefore, it is supposed that this alloy has different creep deformation behaviour at high temperature from the first and second generation SX superalloys. In the present study, we investigated the creep deformation behaviour of the Re-free SX superalloy at high temperature.

2. Experimental procedure

The alloy LSC-15(Ni-6.0Co-7.0Cr-1.5Mo-10.0W-6.0Al-5.5Ta-0.1Hf wt. %) was investigated in this paper. The alloy does not include Rhenium and has been developed by IHI Corporation Japan. The single-crystal superalloy in the fully heat-treated condition was provided by IHI

^a Corresponding author: nobuyasu_tsuno@ihi.co.jp

This is an Open Access article distributed under the terms of the [Creative Commons Attribution License 4.0](https://creativecommons.org/licenses/by/4.0/), which permits unrestricted use, distribution, and reproduction in any medium, provided the original work is properly cited.

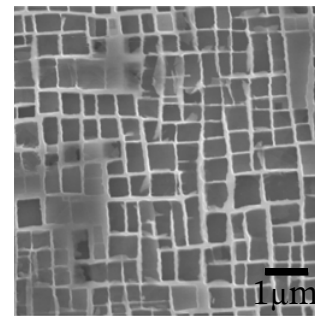


Figure 1. Fully heat treated microstructure of LSC-15.

casting Co. Ltd. Creep tests were performed at 1000 °C and 1050 °C under several stresses. The misorientation of stress direction in each specimen was within 10 ° of [001]. The microstructure of the creep specimens was observed by Scanning Electron Microscope (SEM) and Transmission Electron Microscope (TEM). Thin plates were cut from the crept specimens parallel to longitudinal (110) planes to observe the microstructure evolution by SEM. These plates were mechanically polished and then etched in a γ' dissolving agent prior to SEM observations. The thin foils for TEM analysis were obtained by cutting discs from the gage length perpendicular to the tensile axis. These were electro-polished using a twin jet with a solution of 10% perchloric acid in ethanol at 30 V and 0 °C.

3. Results and discussion

The microstructure of the alloy after aging heat treatment is shown in Fig. 1. The microstructure of alloy has homogeneous distribution of cuboidal primary γ' .

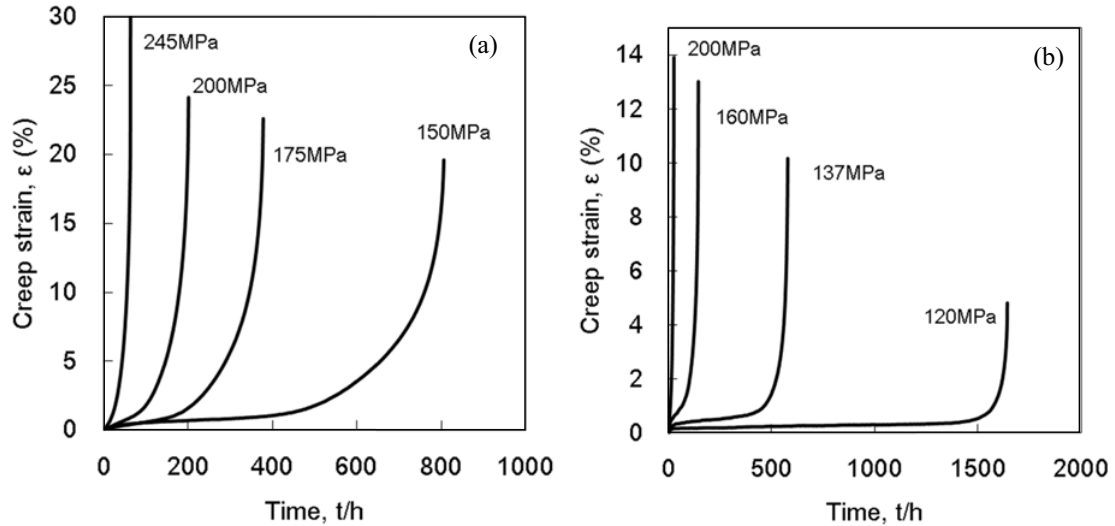


Figure 2. Creep curves from LSC-15 tested at (a) 1000 °C and (b) 1050 °C under several stresses.

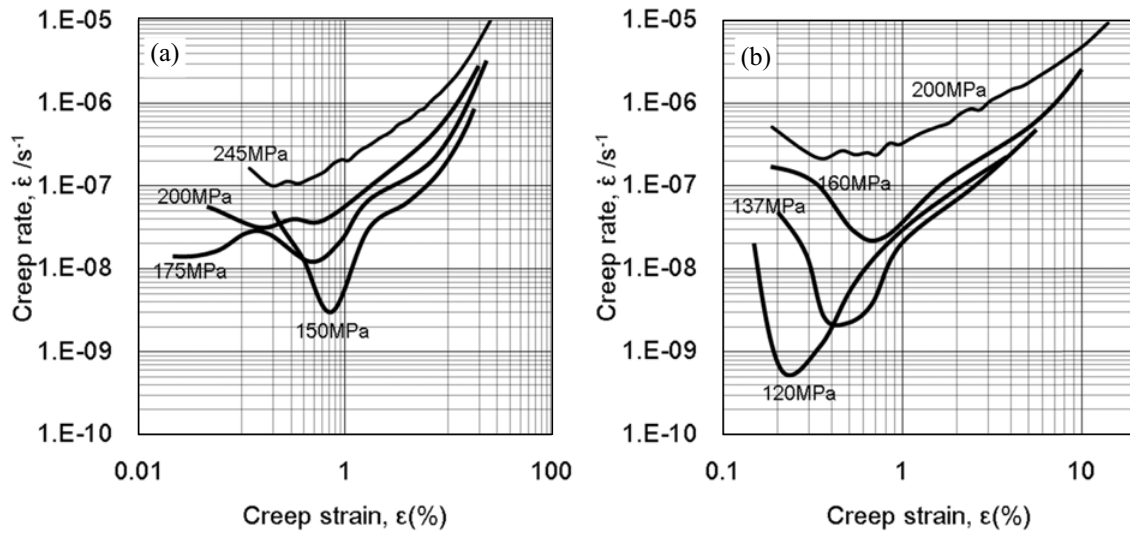


Figure 3. Creep rate-strain curve in LSC-15 at (a) 1000 °C and (b) 1050 °C under several stresses.

The mean γ' edge length was approximately $0.7 \mu\text{m}$. The volume fraction of primary γ' was approximately 70 vol.%. Figure 2 shows creep curves at 1000 °C and 1050 °C. The creep rate-strain curves were shown in Fig. 3. The creep deformation behaviours were different between test temperatures at 1000 °C and 1050 °C. At 1000 °C, the creep strains to reach the minimum creep rate did not depend on the testing stress level. After reaching the minimum creep rate, creep rates increased gradually to rupture. On the other hands, at 1050 °C, the creep strains at minimum creep rate depended on the testing stress. After reaching the minimum creep rate, creep rates increased gradually as well as the curves at 1000 °C. But, creep strain increased rapidly at the final creep region.

When creep properties at 1050 °C were compared between the second generation superalloy and Re-free SX superalloy, rupture times are at the same level. On the other hands, when they are compared at 1000 °C, the creep strength of the Re-free SX superalloy was lower than that of the second generation SX superalloys. Figure 4 shows

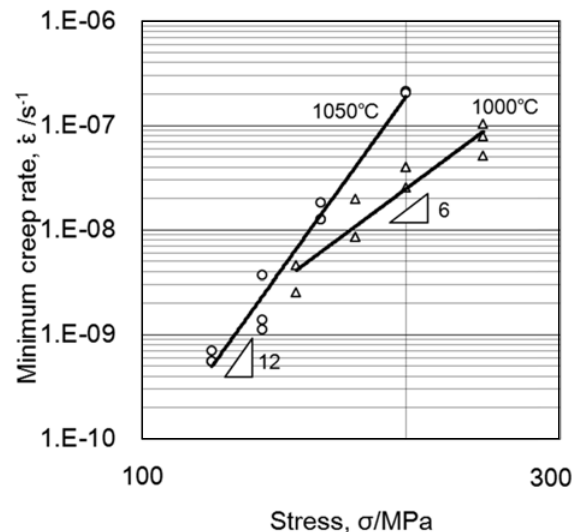


Figure 4. The stress dependence of the minimum creep rate of LSC-15 at two temperatures.

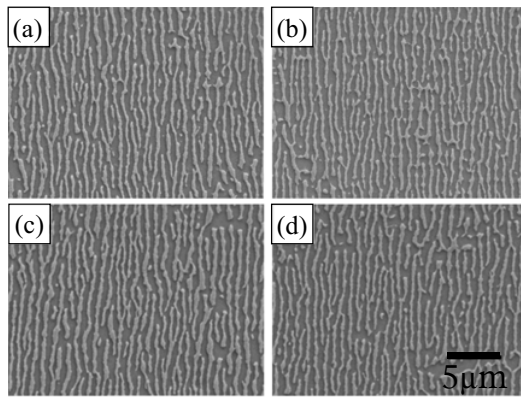


Figure 5. The microstructure of interrupted crept specimens at minimum creep rate; (a) 1000 °C/150 MPa, (b) 1000 °C/175 MPa, (c) 1050 °C/137 MPa, (d) 1050 °C/160 MPa.

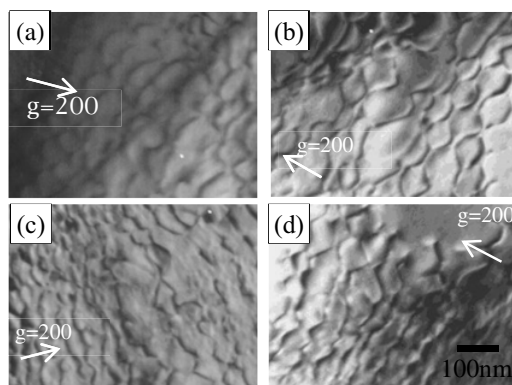


Figure 6. The γ/γ' interfacial dislocation network of interrupted crept specimens; (a) 1000 °C/150 MPa, (b) 1000 °C/175 MPa, (c) 1000 °C/137 MPa, (d) 1050 °C/160 MPa.

Table 1. The γ and γ' width of interrupted crept specimens.

Temperature (°C)	Stress (MPa)	γ width (μm)	γ' width (μm)
1050	137	0.284	0.413
	160	0.292	0.415
1000	150	0.284	0.419
	175	0.296	0.479

the relationship between the minimum creep rate and stress at the various temperatures. Figure 4 shows the difference of stress exponent n -value at 1000 °C and 1050 °C, $n = 6$ and 12 respectively. Therefore, the creep deformation mechanisms are different in the minimum creep region between at the two temperatures. In order to investigate the creep deformation mechanism at the each temperature, the creep test was interrupted at the minimum creep rate and the microstructures were observed by SEM and TEM.

The interrupted tests conditions were 1000 °C/150 MPa, 1000 °C/175 MPa, 1050 °C/137 MPa and 1050 °C/160 MPa. Figure 5 shows that the microstructures of the interrupted crept specimens by SEM. All specimens had γ/γ' rafted structures. The γ and γ' size were summarised in Table 1. These sizes were also the same among the specimens. The γ/γ' interface microstructures of the interrupted crept specimens are shown in Fig. 6. All crept

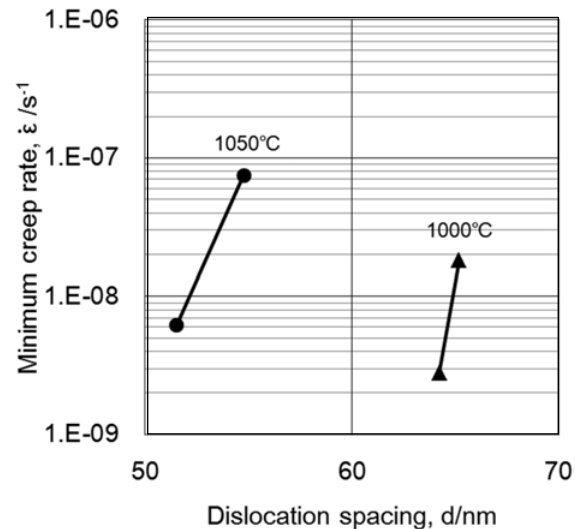


Figure 7. The relationship of γ/γ' interfacial dislocation spacing and minimum creep rate.

specimens had dense interfacial dislocation networks at the γ/γ' interfaces. The relationship between the interfacial dislocation spacing and the minimum creep rate was shown in Fig. 7. The minimum creep rate decreases with the decrease of dislocation spacing in the γ/γ' interface at each temperature. Zhang et al. [5] described the relationship between the interfacial dislocation spacing, minimum creep rate and γ/γ' lattice misfit at high temperature under low stress creep deformation. In the present study, the interfacial dislocation spacing at the corresponding minimum creep rate at 1000 °C and at 1050 °C were different. The creep rate increased with increasing dislocation spacing at 1050 °C, but although it changed at 1000 °C the dislocation spacing did not change at the various stress levels. This suggests that the dislocation network contributes to the creep strength at 1050 °C but does not work effectively at 1000 °C. In Fig. 3, the creep strains at the minimum creep strain rates at the various stress level are almost the same at 1000 °C. This suggests that the similar dislocation network developed and dislocation densities reached the same level at the minimum creep rates in the creep tests at the various stresses. Then, solid solution strength might be effective on creep strength in 1000 °C. On the other hand, creep strain at minimum creep rate depends on stress level at 1050 °C. It suggests that dislocation network development at the minimum creep rate changes with stress level at this temperature. Because the solid solution strengthening element at 1000 °C is more effective than at 1050 °C, the creep rate at 1050 °C could reach at the minimum creep rate at an earlier stage than at 1000 °C. Therefore, dislocation network had not developed fully at the minimum creep rate and the specimens crept in the shorter test duration under the higher stress at 1050 °C. It is considered that n value shows 6 because amounts of dislocation network strength are the same at 1000 °C even though the stress levels were different. The value of n at 1050 °C is 12, higher than at 1000 °C because the dislocation network strength is prior to solid solution strength at 1050 °C.

4. Conclusions

The following conclusions were obtained in this study:

1. The creep deformation behaviours at 1000 °C and 1050 °C in LSC-15 are different.
2. At 1000 °C, n value shows 6 the creep strength by dislocation network is not dominant. On the other hand, n value shows 12 the creep strength by dislocation network is dominant. Then, stress dependency at 1050 °C is higher than that at 1000 °C.

References

- [1] A. D. Cetel, D. N. Duhal, *Superalloys* 1988, 235 (1988)
- [2] K. Harris, G.L. Erickson, S.L. Sikkenga, W.D. Brentanall, J.M. Aurrecoechea, K.G. Kubarych, *Superalloys* 1992, 297 (1992)
- [3] G.L. Erickson, *Superalloys* 1996, 35 (1996)
- [4] W.S. Walston, L.S. O'Hara, E.W. Ross, T.M. Pollock, W.H. Murphy, *Superalloys* 1996, 27 (1996)
- [5] J.X. Zhang, T. Murakumo, Y. Koizumi, T. Kobayashi, H. Harada, S. Masaki, Jr. *Metall. Mater. Trans. A*, **33A**, 3741 (2002)
- [6] Y. Koizumi, T. Kobayashi, T. Yokokawa, J. Zhang, M. Ogawa, H. Harada, Y. Aoki, M. Arai, *Superalloys* 2004, 35 (2004)
- [7] P.J. Fink, J.L. Miller, D.G. Konitzer, *JOM*, **62**, 55 (2010)
- [8] J.B. Wahl, K. Harris, *Superalloys* 2012, 179 (2012)